

# Apolipoprotein E4 Forms a Molten Globule

A POTENTIAL BASIS FOR ITS ASSOCIATION WITH DISEASE\*

Received for publication, May 17, 2002, and in revised form, October 21, 2002  
Published, JBC Papers in Press, October 21, 2002, DOI 10.1074/jbc.M204898200

Julie A. Morrow<sup>‡§¶</sup>, Danny M. Hatters<sup>‡§¶</sup>, Bin Lu<sup>‡§</sup>, Peter Höcht<sup>||</sup>, Keith A. Oberg<sup>\*\*</sup>,  
Bernhard Rupp<sup>||</sup>, and Karl H. Weisgraber<sup>‡§¶§§</sup>

From the <sup>‡</sup>Gladstone Institutes of Cardiovascular Disease and Neurological Disease, San Francisco, California 94141-9100, the <sup>§</sup>Cardiovascular Research Institute and the <sup>¶¶</sup>Department of Pathology, University of California, San Francisco, California 94143, <sup>||</sup>Lawrence Livermore National Laboratory, Livermore, California 94551, and <sup>\*\*</sup>Allecure, Inc., Los Angeles, California 91355

The amino-terminal domain of apolipoprotein (apo) E4 is less susceptible to chemical and thermal denaturation than the apoE3 and apoE2 domains. We compared the urea denaturation curves of the 22-kDa amino-terminal domains of the apoE isoforms at pH 7.4 and 4.0. At pH 7.4, apoE3 and apoE4 reflected an apparent two-state denaturation. The midpoints of denaturation were 5.2 and 4.3 M urea, respectively. At pH 4.0, a pH value known to stabilize folding intermediates, apoE4 and apoE3 displayed the same order of denaturation but with distinct plateaus, suggesting the presence of a stable folding intermediate. In contrast, apoE2 proved the most stable and lacked the distinct plateau observed with the other two isoforms and could be fitted to a two-state unfolding model. Analysis of the curves with a three-state unfolding model (native, intermediate, and unfolded) showed that the apoE4 folding intermediate reached its maximal concentration (~90% of the mixture) at 3.75 M, whereas the apoE3 intermediate was maximal at 4.75 M (~80%). These results are consistent with apoE4 being more susceptible to unfolding than apoE3 and apoE2 and more prone to form a stable folding intermediate. The structure of the apoE4 folding intermediate at pH 4.0 in 3.75 M urea was characterized using pepsin proteolysis, Fourier transform infrared spectroscopy, and dynamic light scattering. From these studies, we conclude that the apoE4 folding intermediate is a single molecule with the characteristics of a molten globule. We propose a model of the apoE4 molten globule in which the four-helix bundle of the amino-terminal domain is partially opened, generating a slightly elongated structure and exposing the hydrophobic core. Since molten globules have been implicated in both normal and abnormal physiological function, the differential abilities of the apoE isoforms to form a molten globule may contribute to the isoform-specific effects of apoE in disease.

involved in the maintenance and repair of neurons (1, 2). One of the common human apoE isoforms, apoE4, is a major risk factor for Alzheimer's disease (3–5) and atherosclerosis (6–8). ApoE4 is also associated with poor recovery from head injury and stroke (9–11), cognitive decline associated with coronary bypass surgery (12), increased severity of tissue damage in multiple sclerosis (13), shortening of survival after the onset of amyotrophic lateral sclerosis (14), and a poor response to other forms of central nervous system stress (15).

The three common isoforms of apoE (apoE2, apoE3, and apoE4) are genetically determined and differ in cysteine and arginine content at positions 112 and 158: apoE2 (Cys<sup>112</sup>, Cys<sup>158</sup>), apoE3 (Cys<sup>112</sup>, Arg<sup>158</sup>), and apoE4 (Arg<sup>112</sup>, Arg<sup>158</sup>) (16, 17). The protein contains two distinct structural domains: a 22-kDa amino-terminal domain and a 10-kDa carboxyl-terminal domain (18, 19). In apoE4 and not the other isoforms, the two domains interact in a unique manner. In apoE4, Arg<sup>112</sup> causes Arg<sup>61</sup> to assume a unique conformation and interact with Glu<sup>255</sup> in the carboxyl-terminal domain. This novel property of apoE4 is referred to as apoE4 domain interaction (20, 21) and was suggested to contribute to the association of apoE4 with disease (2, 21).

Previously, we demonstrated that the two domains of apoE unfold independently for all three isoforms (19, 22) and that the 22-kDa fragments, which contain the amino acid interchanges, differ in their susceptibility to thermal and chemical denaturation (apoE4 < apoE3 < apoE2) (22, 23). Denaturation of apoE2 with guanidine at neutral pH displayed two-stage cooperative unfolding, whereas apoE3 and apoE4 displayed noncooperative unfolding that was much more prominent with apoE4. This noncooperative unfolding of apoE4 suggested the presence of a stable folding intermediate (22).

Folding intermediates that are both stable under certain conditions and have nearly native structural features are referred to as molten globules (24). Three structural features characterize the molten globule state. First, a significant amount of secondary structure of the native state is retained. Second, although there is considerable loss of tertiary structure, the molten globule is structurally compact. Third, there is internal mobility with exposure of the hydrophobic core. Until recently, it was assumed that the molten globule was a relatively rare state for a protein. However, there is increasing evidence that molten globules are common and that they play a key role in a wide variety of physiological processes, including translocation across membranes, increased affinity for membranes, binding to liposomes and phospholipids, protein traf-

Apolipoprotein (apo)<sup>1</sup> E plays a key role in lipid transport throughout the body including the nervous system and is in-

\* This work was supported in part by grant NS35939 from the National Institutes of Health (to K. H. W.). The costs of publication of this article were defrayed in part by the payment of page charges. This article must therefore be hereby marked "advertisement" in accordance with 18 U.S.C. Section 1734 solely to indicate this fact.

¶ Both authors contributed equally to this work.

§§ To whom correspondence should be addressed: Gladstone Inst. of Cardiovascular Disease, P. O. Box 419100, San Francisco, CA 94141-9100. Tel.: 415-826-7500; Fax: 415-285-5632; E-mail: kweisgraber@gladstone.ucsf.edu.

<sup>1</sup> The abbreviations used are: apo, apolipoprotein; FTIR, Fourier transform infrared spectroscopy; DLS, dynamic light scattering;

DMPC, dimyristoylphosphatidylcholine;  $R_h$ , hydrodynamic radius;  $M_r$ , molecular mass.

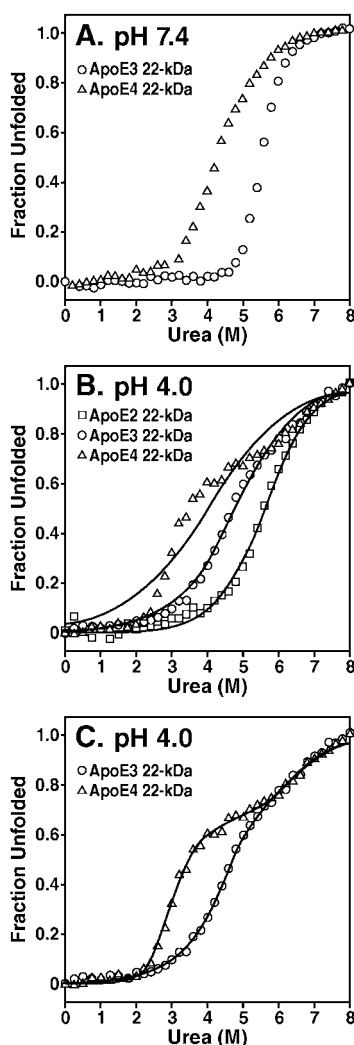


FIG. 1. Urea denaturation of apoE 22-kDa fragments. The unfolding of the apoE3 and apoE4 fragments at various urea concentrations at pH 7.4 (A) and for the apoE2, apoE3, and apoE4 fragments at pH 4.0 (B) was monitored by circular dichroism. The solid lines indicate fits to a two-state model (B) or a three-state model (C).

ficking, extracellular secretion, and the control and regulation of the cell cycle (24, 25). Indeed, apolipoproteins, including human apoA-I and insect apolipophorin III, have also been reported as molten globules (26, 27). In these cases, it was proposed that internal mobility provides structural plasticity for binding to lipoprotein surfaces (26, 27).

In this report, we demonstrate that apoE4 forms a stable folding intermediate more readily than apoE3 and apoE2. Using a variety of structural tools to characterize its structure, including pepsin proteolysis, Fourier transform infrared spectroscopy (FTIR), and dynamic light scattering (DLS), we show that this stable apoE4 folding intermediate possesses the structural characteristics of a molten globule. We conclude that, in addition to apoE4 domain interaction, the propensity of apoE4 to form a molten globule may contribute to its association with disease.

#### EXPERIMENTAL PROCEDURES

**Urea Denaturation**—The 22-kDa fragments of apoE were expressed recombinantly in bacteria and purified as described (22). Protein (400  $\mu$ g/ml) was incubated overnight at 4 °C in buffer, 1 mM dithiothreitol, and freshly deionized urea at various concentrations. The buffer was 10 mM sodium phosphate for experiments at pH 7.4 and 20 mM sodium acetate for experiments at pH 4.0, which maintained the same ionic strength for both experiments. Circular dichroism measurements were

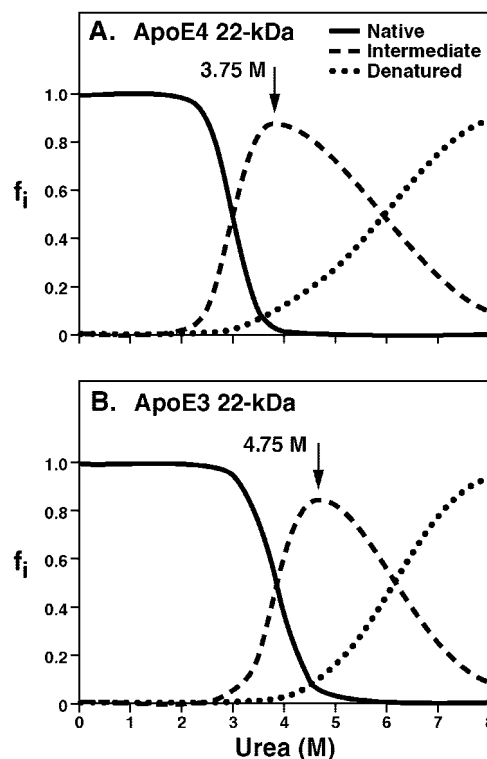


FIG. 2. Urea denaturation curves of the 22-kDa fragments of apoE3 and apoE4 at pH 4.0. The curves were analyzed by using a three-state model to determine the fraction of native (solid line), intermediate (dashed line), and unfolded (dotted line) structures at various urea concentrations.

made on a Jasco 715 or Applied Biophysics  $\pi$ -180 spectropolarimeter using a 1-mm pathlength cuvette. All experiments were performed under reducing conditions (5 mM dithiothreitol) at 25 °C. Molar ellipticity ( $[\theta]$ ) at 220 nm was calculated from the relationship  $[\theta] = (\text{MRW})(\theta_{220})/(10)(l)(c)$ , where  $\theta_{220}$  is the measured ellipticity at 220 nm in degrees,  $l$  is the cuvette pathlength (0.1 cm),  $c$  is the protein concentration in g/ml, and the mean residue weight (MRW) was 114. The denaturation curves at pH 4.0 were analyzed according to a two- or three-state model as previously described (28).

**Proteolysis of the 22-kDa Fragment of ApoE**—Pepsin (Sigma) was added to the 22-kDa fragment of apoE (0.1 mg/ml, 20 mM sodium acetate, pH 4.0) in 0, 3.75, or 4.75 M urea at a ratio of 10:1, 250:1, or 2000:1 (apoE:pepsin, w/w), respectively, and incubated at room temperature. At various time points, 500- $\mu$ l aliquots were taken. Tris buffer and NaOH were added to inactivate pepsin, and the sample was dialyzed against 100 mM ammonium bicarbonate to remove the urea before lyophilization of the sample. The sample was then resuspended in a Tris-Tricine sample buffer and analyzed by SDS-PAGE followed by transfer to a polyvinylidene fluoride membrane for amino-terminal sequencing (PerkinElmer Life Sciences Precise protein sequencer).

**Analysis of the 22-kDa Fragment of ApoE4 by Infrared Spectroscopy**—Solution-attenuated total reflectance FTIR was performed on the 22-kDa fragment of apoE4 (10 mg/ml, 10 mM cacodylate, pH 4.0, with or without 3.75 M urea) as described (29). The spectra were analyzed to estimate secondary structural content as described (30, 31).

**DLS**—Scattering data were collected at 20 °C with a DynaPro-MS/X (Protein Solutions). Samples of the apoE4 22-kDa fragment (0.5 mg/ml) were examined at pH 7.4 and 4.0 in the absence of urea and at pH 4.0 in the presence of 3.75 M urea. Diffusion coefficients were determined from scattering data with the DYNAMICS autocorrelation analysis software (version 5.25.44, Protein Solutions). All data could be fitted multimodally, and essentially 100% of the scattering mass was attributed to a single low molecular mass component. The diffusion coefficient ( $D$ ) and the hydrodynamic radius ( $R_h$ ) are related by  $R_h = kT/6\pi\eta D$ . Viscosity ( $\eta$ ) for the dilute sodium-acetate buffer was set to 1.0. The molecular mass ( $M_r$ ) was estimated from the empirical relation  $M_r = (R_h/k)^n$ , where  $k$  and  $n$  are parameters specific for the hydrodynamic model used. For globular proteins,  $k = 1.68$  and  $n = 2.34$ . For nonspherical proteins, the  $R_h$  must be corrected by using the Perrin

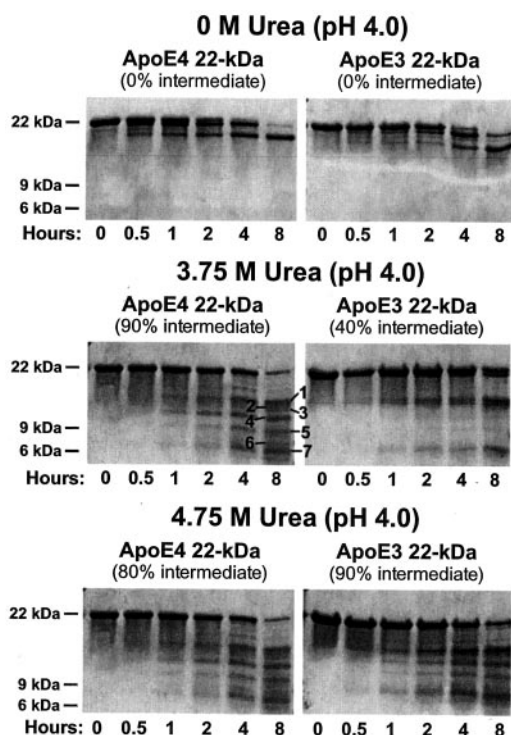


FIG. 3. Pepsin proteolysis as a probe of the conformation of apoE3 and apoE4. The 22-kDa fragments of apoE3 and apoE4 were subjected to limited pepsin digestion in the presence and absence of urea at pH 4.0, and the extent of fragmentation was monitored by SDS-PAGE.

factor  $F$  determined from molecular dimensions. The apoE4 22-kDa fragment was approximated as a prolate ellipsoid with an axial ratio of 1:2.5 ( $F \approx 1.08$ ). The pullulan model (an extended polysaccharide) was used to estimate hydrodynamic properties for random conformations ( $k = 1.48$ ,  $n = 1.81$ ). The derivations of the equations we used to calculate hydrodynamic properties are reviewed in Ref. 32.

**Turbidimetric DMPC Clearance Assay**—The kinetics of dimyristoylphosphatidylcholine (DMPC) large multilamellar vesicle remodeling was performed as described (33) with slight modifications. Samples of apoE 22-kDa fragments were dialyzed into 5 mM dithiothreitol, 20 mM sodium acetate, pH 4.0, containing either 3.75 or 4.75 M urea at 4 °C and adjusted to a final protein concentration of 0.5 mg/ml. A solution of DMPC (Avanti Polar Lipids) in chloroform:methanol (1:1, v/v) was evaporated under a stream of argon and further desiccated under reduced pressure overnight. The dried DMPC film was resuspended in 20 mM sodium acetate, pH 4.0, containing either 3.75 or 4.75 M urea. The concentration of DMPC was determined using an enzymatic colorimetric assay for phospholipids (Wako Chemicals) and diluted to a final DMPC concentration of 0.5 mg/ml. DMPC solution (400  $\mu$ l) was added to a 1-cm pathlength quartz cuvette followed by the addition of buffer or protein solution with rapid mixing (200  $\mu$ l). The turbidity of the solution was monitored at a wavelength of 325 nm using a Beckman DU-640 spectrophotometer. All solutions were maintained at a temperature of 24 °C before mixing and during data collection.

## RESULTS

To follow up on our previous guanidine denaturation studies that suggested the presence of an apoE4 folding intermediate (22), the 22-kDa fragments of apoE3 and apoE4 were examined by urea denaturation at pH 7.4 and pH 4.0 since low pH facilitates the formation of stable folding intermediates (molten globules). The denaturation curves at pH 7.4 reflected an apparent two-state denaturation. The midpoints of denaturation for the 22-kDa fragments of apoE3 and apoE4 were 5.2 and 4.3 M urea, respectively, consistent with previous results (22) (Fig. 1A). At pH 4.0, apoE4 and apoE3 displayed the same order of denaturation (apoE4 > apoE3). However, there was a distinct plateau in the curves for both isoforms, suggesting the presence of a stable folding intermediate (Fig. 1B). As with guanidine

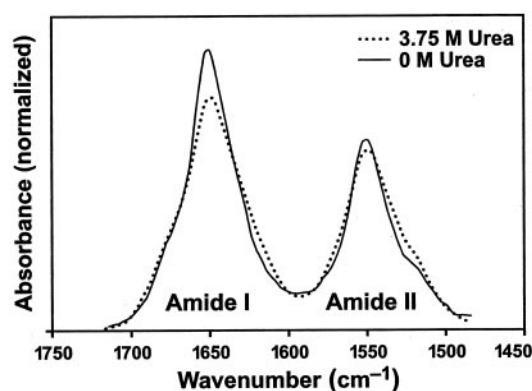


FIG. 4. FTIR analysis of apoE4 22-kDa fragment. Analysis in the amide I and II regions of the spectra was performed in the absence and presence of urea. The analysis in the absence of urea represents a single determination; the estimate of 75%  $\alpha$ -helix is in excellent agreement with the x-ray crystal structure (34). The analysis in the absence of urea was performed in duplicate with results in 3% agreement.

TABLE I  
Hydrodynamic radius and derived properties for the apoE4 22-kDa fragment

pH [urea] (M)	7.4 0.0	4.0 0.0	4.0 3.75
Hydrodynamic radius (nm, e.s.u.)	$2.40 \pm 0.47$	$2.61 \pm 0.67$	$3.93 \pm 0.4$
Polydispersity (%) <sup>a</sup>	19.5	25.5	12.5
$M_r$ (kDa, globular estimate)	26.1	31.7	82.8
$M_r$ (kDa, $\alpha$ shape corrected) <sup>b</sup>	21.8	26.5	24.2

<sup>a</sup> Polydispersity is a measure of the size distribution.

<sup>b</sup> Prolate ellipsoid shape correction factor  $f = 1.08$  used in calculation for columns 1 and 2. A random coil model was used for the calculation of  $M_r$  in column 3.

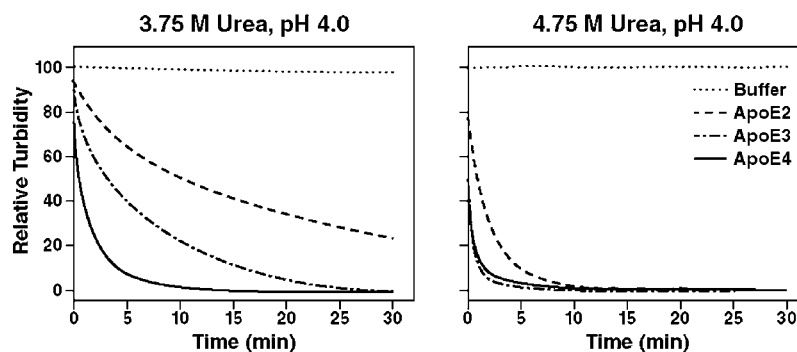
denaturation, apoE2 was the most resistant to unfolding in urea and lacked an obvious plateau indicating that it did not form a folding intermediate (Fig. 1B.) The data in Fig. 1B were fitted to a 2-state model (unfolded/folded, solid lines overlaying the data). The poor fits to the apoE3 and apoE4 data further highlight the presence of stable folding intermediates in comparison to the reasonable fit obtained for the apoE2 data. Therefore, the data were analyzed according to a three-state model (native/intermediate/unfolded) (28), which gave excellent fits for the apoE3 and apoE4 isoforms (Fig. 1C) but did not give a better fit for apoE2 than the two-state model. Fig. 2 shows the fractions of folded, intermediate, and unfolded protein for apoE3 and apoE4, according to the three-state model. The concentration of urea at which the folding intermediate was at maximum concentration was 3.75 M for the apoE4 22-kDa fragment ( $\approx 90\%$ ) and 4.75 M for the apoE3 fragment ( $\approx 80\%$ ). These results demonstrate that in urea the folding intermediate is a stable thermodynamic state, the first criterion for a molten globule.

**Pepsin Proteolysis**—Since proteolysis is a sensitive probe for conformational changes in proteins (33), the apoE fragments were subjected to limited proteolysis with pepsin at low pH with or without urea and analyzed by SDS-PAGE and amino-terminal sequencing. In 0 M urea, there was one major fragment, which had the amino-terminal sequence of RQQTE, which corresponds to amino acids 15–19 in apoE (Fig. 3, top panels). This sequence is at the flexible amino terminus of the 22-kDa fragment that is not resolved in the x-ray structure (34). Further addition of pepsin or longer digestion times did not produce smaller cleavage products under these conditions.

Digestion of the apoE4 22-kDa fragment in 3.75 M urea, the concentration at which the intermediate represents  $\approx 90\%$  of



FIG. 5. Comparison of the lipid-binding activities of the apoE2, apoE3, and apoE4 22-kDa fragments at pH 4.0. The relative abilities of the fragments to clear DMPC vesicles were determined in a turbidimetric clearing assay in the presence of 3.75 and 4.75 M urea where the population of intermediate species is highest for apoE3 and apoE4, respectively. Clearance curves are representative of three independent experiments.



the mixture, revealed seven major bands (Fig. 3, *middle panels*). Bands 1–5 had the amino-terminal sequence GS<sup>1</sup>KVE, the same as that of recombinant apoE (it contains the novel Gly-Ser sequence at the amino terminus) (35). Band 4 also contained a fragment with the amino-terminal sequence <sup>79</sup>EE-QLTP. Band 6 had the amino-terminal sequence <sup>122</sup>VQYRG. Band 7 was rather broad and contained three fragments (<sup>124</sup>AMLGQSTEE, <sup>133</sup>RVRLASHLR, and <sup>116</sup>VQYRGEVQA). Digestion of the apoE3 22-kDa fragment in 3.75 M urea yielded the same bands as the apoE4 digestion but with less proteolysis of the intact apoE3 fragment (Fig. 3, *middle panels*).

The bands after digestion of apoE3 and apoE4 in 4.75 M urea were similar to those obtained after digestion in 3.75 M urea, but there was less difference in the extent of digestion (Fig. 3, *bottom panels*). This result is consistent with the prediction, based on analysis of a three-state model, that similar amounts of the intermediate states from each isoform would be present in 4.75 M urea but not in 3.75 M urea. The increased sensitivity to pepsin digestion is also consistent with an altered conformation at low pH in the presence of urea, another characteristic of a molten globule. It is also important to note that there are a limited number of exposed pepsin cleavage sites, which is consistent with a limited structural or conformational reorganization of the apoE4 intermediate without complete loss of native structure.

**FTIR**—Since it is difficult to accurately estimate the secondary structure of a protein in urea by far ultraviolet circular dichroism due to the high absorbance of urea below 210 nm, we used a novel FTIR method to assess the secondary structure of the intermediate in urea. This method includes the subtraction of the urea background, as well as subtraction of absorbed (partially denatured) protein (29). The apoE4 22-kDa fragment was analyzed at pH 4.0 in the presence or absence of 3.75 M urea (Fig. 4). ApoE4 22-kDa in 0 M urea displayed 75%  $\alpha$ -helix and 3%  $\beta$ -sheet, consistent with the  $\alpha$ -helical content estimated by circular dichroism (18) and x-ray crystallography (34). In 3.75 M urea, apoE4 22-kDa displayed 46%  $\alpha$ -helix and 17%  $\beta$ -sheet. Thus, the intermediate retains 61% of the native helical content, another criterion of a molten globule. In addition, it has a significant increase in  $\beta$  structure, which has implications for promoting aggregation and fibrillization.

**DLS**—DLS was used to determine the aggregation state of the intermediate. The measured hydrodynamic radii and estimated molecular masses are summarized in Table I. The shape-corrected  $M_r$  calculated for the reference sample apoE4 22-kDa fragment at pH 7.4 with no urea was 22 kDa. At pH 4.0 (no urea), the size distribution (polydispersity) was wider, and the  $R_h$  was larger. Although the difference was not significant within the error of the experiment, it is reasonable to speculate that both the larger  $R_h$  and the greater size distribution indicate a somewhat lower stability of the apoE4 22-kDa fragment at the acidic pH, consistent with its increased tendency to form an intermediate at pH 4.0. A small widening in the flexible and

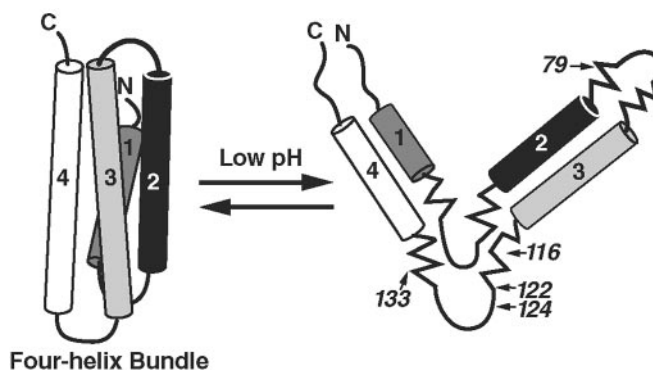


FIG. 6. Model of the apoE4 22-kDa fragment in its molten globule state. Based on the structural and physical characterization of the apoE4 molten globule, we propose that at pH 4.0 the four-helix bundle of apoE is partially open, generating a slightly elongated structure in which there is a shortening of the  $\alpha$ -helices and an increase in  $\beta$  structure at the ends of the helices. The peptic cleavage sites that are exposed in the molten globule state (Fig. 3) are indicated by the small arrows.

dynamic helix bundle, as indicated by crystallographic studies (36), would not lead to a change in the helical content as determined from circular dichroism spectra and thus would still be compatible with a small increase in the  $R_h$ , indicating a flexing of the four-helix bundle at pH 4.0.

A more dramatic change was observed in the hydrodynamic behavior of the apoE4 22-kDa fragment at pH 4.0 in 3.75 M urea.  $R_h$  increased significantly, but the size distribution remained narrow, indicating a well-defined intermediate species. Assuming a large contribution of random coil conformation in the intermediate, the  $M_r$  corresponding to the  $R_h$  for a random coil model was estimated to be  $\approx 24$  kDa, consistent with a monomeric species and no evidence of aggregation under these conditions.

**Lipid Binding Abilities of the Three Isoforms**—Since molten globules have been implicated in membrane association and phospholipid binding (37), the relative abilities of the three isoforms to bind and disrupt DMPC vesicles were determined at pH 4.0 in a turbidimetric clearing assay under urea concentrations where the intermediate species is highly populated for apoE4 and apoE3. It is important to note that while the carboxyl-terminal domain of apoE contains the major lipid binding determinants, the N-terminal 22-kDa domain also is capable of binding to lipid. Previous studies have indicated that the N-terminal 22-kDa fragment clears at approximately half the rate of the intact protein at pH 7.4 (38). In the presence of 3.75 M urea, where the apoE4 22-kDa fragment has its maximum population of intermediate species ( $\approx 90\%$ ), apoE4 is more effective in clearing DMPC solutions than both apoE3 and apoE2 (Fig. 5). In 4.75 M urea, where apoE3 has its maximum population of intermediate species ( $\approx 80\%$ ) and apoE4 is close to its maximum population ( $\approx 80\%$ ), apoE3 and apoE4 have a similar

rate of clearance, while apoE2 lags behind. At 4.75 M urea, the relative clearance rate of apoE2 is closer to that of apoE4 and apoE3 than at 3.75 M urea. There are two reasons for this. First, the DMPC vesicles are smaller at 4.75 M urea than at 3.75 M, based on their relative scattering intensities. Thus, the lipid substrate is different at the two urea concentrations. Second, at 4.75 M urea, the apoE2 is beginning to unfold, which would be predicted to increase its lipid-binding ability. The important point is that apoE2 still lags behind apoE4 and apoE3, which is consistent with its greater stability and absence of any significant concentration of a folding intermediate. Overall, the results are consistent with the enhanced ability of the intermediate species to remodel DMPC compared with the folded state.

#### DISCUSSION

This study shows that the folding intermediate of apoE4 can be stabilized and its structure characterized at pH 4.0 in 3.75 M urea. Pepsin digestion revealed that, in forming the intermediate, apoE4 undergoes a conformational change that involves opening of the four-helix bundle. FTIR analysis demonstrates that the intermediate retains much of its secondary structure (61%), with a modest increase in  $\beta$  structure. The DLS results indicate that the intermediate is a single molecule with a narrow polydispersity and slightly elongated structure. These structural properties of the apoE4 intermediate are consistent with those of a molten globule. Based on our structural characterization, we propose a model for the apoE4 molten globule (Fig. 6). The bundle is partially open, generating a slightly elongated structure and exposing the hydrophobic core (DLS and pepsin digestion data), and most of the  $\alpha$ -helical structure is retained (FTIR and pepsin cleavage data). We suggest that the helical structure is lost at the end of the helices where it is converted to  $\beta$  structure or random structure, exposing the pepsin cleavage sites.

The largely opened conformation of the four-helix bundle in the intermediate is similar to the conformation change of apoE when it binds to lipid (36, 37, 39, 40). The DLS data are consistent with an intermediate consisting of short ( $\approx 20$  Å) helical segments or building blocks of the stable domain, tethered by long segments containing random coil and  $\beta$  structure. Although it is difficult to estimate accurately the hydrodynamic parameters of the intermediate model, it is reasonable to assume that such a chain of tethered helical segments would display very much the behavior we observe for the folding intermediate.

The emerging view is that molten globules play an important role in many physiological processes, including translocation across membranes, increased affinity for membranes, binding to liposomes and phospholipids, protein trafficking, extracellular secretion, and the control and regulation of the cell cycle (24, 25). It has been suggested that the molten globule state is the rule rather than the exception and that it actually represents the third thermodynamic state that a protein can assume. Protein structures are not static, and it is highly likely that proteins undergo conformational changes in performing their normal functions. Thus, molten globules are ideally suited to provide this conformational flexibility. With apolipoproteins, molten globules may be particularly important in providing structural flexibility given that studies on the apoE3 22-kDa fragment and apolipoprotein III reveal a correlation between faster phospholipid clearance rates and low pH and a less defined tertiary structure (27, 41).

However, protein mutations that affect molten globule formation may also adversely affect normal physiology. Such mutations may destabilize the molten globule, facilitate its formation, or trap it in this state, preventing native folding. For

example, the mislocation of the cystic fibrosis transmembrane conductance regulator is suggested to involve a molten globule (24). A change in a single amino acid residue causes it to form a stable complex with the chaperone heat shock protein-70. This complex is retained in the endoplasmic reticulum, preventing it from reaching its normal location in the plasma membrane.

The greater propensity of apoE4 than apoE3 or apoE2 to form a molten globule has potential implications in lipoprotein metabolism, neuronal maintenance, and neurodegeneration, including Alzheimer's disease. ApoE transports and redistributes lipid in both the plasma and central nervous system (1), and apoE3- and apoE4-containing lipoproteins have different effects on neurite outgrowth in cultured neurons: apoE3 promotes, whereas apoE4 inhibits neurite extension (42–48). These results led to the hypothesis that apoE participates in the normal maintenance of neurons and in neuronal repair in response to central nervous system injury and that apoE3 is more efficient than apoE4 in these functions (2, 49). These differences may be directly related to how lipids are transported and delivered in an isoform-specific manner in the central nervous system, as well in the plasma. Potentially, molten globule formation could influence lipid binding properties in an isoform-specific manner, as suggested in the DMPC binding assays (Fig. 5).

In addition to apoE4 domain interaction, the apoE4 molten globule may contribute to the apoE isoform-specific effects that have been suggested as mechanisms to explain the association of apoE4 with neurodegeneration. For example, the formation of an apoE4 molten globule within lysosomes or endosomes may result in the interaction of apoE4 with membranes and in the potential of apoE4 to translocate and enter the cytosol where it could disrupt the cytoskeleton (44), promote tau and neurofilament phosphorylation, and induce the formation of intracellular neurofibrillary tangle-like inclusions (50), all features of Alzheimer's disease pathology. Lysosomal disruption and cytoplasmic entry may also explain the apoE4-specific enhancement of A $\beta$ -induced lysosomal leakage and apoptosis when cells are treated with the A $\beta$  peptide in the presence of apoE (51). In addition, the generation of  $\beta$  structure in the molten globule may account for the ability of apoE4 to promote A $\beta$  amyloid fiber formation (52–54) more effectively than apoE3 or to act as a pathological chaperone (55).

In summary, physical and structural characterization of the folding intermediate of the apoE4 amino-terminal domain supports the conclusion that it is a molten globule. The four-helix bundle appears to open partially, generating a flexible species and exposing the hydrophobic core. Since molten globules have been implicated in both the normal and abnormal physiological functions, our working hypothesis is that the differential abilities of the apoE isoforms to form a molten globule also contribute to the known isoform-specific effects in disease.

**Acknowledgments**—We thank Dr. David Dolak (Protein Solutions Inc., Charlottesville, VA) for DLS data collection, Brian Auerbach for manuscript preparation, Gary Howard and Stephen Ordway for editorial assistance, Maryam Tabar for technical assistance, and Jack Hull and John Carroll for graphics. Lawrence Livermore National Laboratory is operated by the University of California for the United States Department of Energy under contract W-7405-ENG-48.

#### REFERENCES

1. Mahley, R. W. (1988) *Science* **240**, 622–630
2. Weisgraber, K. H., and Mahley, R. W. (1996) *FASEB J.* **10**, 1485–1494
3. Strittmatter, W. J., Saunders, A. M., Schmechel, D., Pericak-Vance, M., Enghild, J., Salvesen, G. S., and Roses, A. D. (1993) *Proc. Natl. Acad. Sci. U. S. A.* **90**, 1977–1981
4. Corder, E. H., Saunders, A. M., Strittmatter, W. J., Schmechel, D. E., Gaskell, P. C., Small, G. W., Roses, A. D., Haines, J. L., and Pericak-Vance, M. A. (1993) *Science* **261**, 921–923
5. Saunders, A. M., Strittmatter, W. J., Schmechel, D., St. George-Hyslop, P. H.,

- Pericak-Vance, M. A., Joo, S. H., Rosi, B. L., Gusella, J. F., Crapper-MacLachlan, D. R., Alberts, M. J., Huette, C., Crain, B., Goldgaber, D., and Roses, A. D. (1993) *Neurology* **43**, 1467–1472
6. Utermann, G., Hardewig, A., and Zimmer, F. (1984) *Hum. Genet.* **65**, 237–241
  7. Luc, G., Bard, J.-M., Arveiler, D., Evans, A., Cambou, J.-P., Bingham, A., Amouyel, P., Schaffer, P., Ruidavets, J.-B., Cambien, F., Fruchart, J.-C., and Ducimetiere, P. (1994) *Arterioscler. Thromb.* **14**, 1412–1419
  8. Eichner, J. E., Kuller, L. H., Orchard, T. J., Grandits, G. A., McCallum, L. M., Ferrell, R. E., and Neaton, J. D. (1993) *Am. J. Cardiol.* **71**, 160–165
  9. Mayeux, R., Ottman, R., Maestre, G., Ngai, C., Tang, M.-X., Ginsberg, H., Chun, M., Tycko, B., and Shelanski, M. (1995) *Neurology* **45**, 555–557
  10. Slioter, A. J. C., Tang, M.-X., van Duijn, C. M., Stern, Y., Ott, A., Bell, K., Breteler, M. M. B., Van Broeckhoven, C., Tatemichi, T. K., Tycko, B., Hofman, A., and Mayeux, R. (1997) *J. Am. Med. Assoc.* **277**, 818–821
  11. Teasdale, G. M., Nicoll, J. A. R., Murray, G., and Fiddes, M. (1997) *Lancet* **350**, 1069–1071
  12. Tardiff, B. E., Newman, M. F., Saunders, A. M., Strittmatter, W. J., Blumenthal, J. A., White, W. D., Croughwell, N. D., Davis, R. D., Jr., Roses, A. D., Reves, J. G., and the Neurologic Outcome Research Group of the Duke Heart Center (1997) *Ann. Thorac. Surg.* **64**, 715–720
  13. Fazekas, F., Strasser-Fuchs, S., Schmidt, H., Enzinger, C., Ropele, S., Lechner, A., Flooh, E., Schmidt, R., and Hartung, H.-P. (2000) *J. Neurol. Neurosurg. Psychiatry* **69**, 25–28
  14. Drory, V. E., Birnbaum, M., Korczyn, A. D., and Chapman, J. (2001) *J. Neurol. Sci.* **190**, 17–20
  15. Roses, A. D. (1998) *Ann. N. Y. Acad. Sci.* **855**, 738–743
  16. Weisgraber, K. H., Rall, S. C., Jr., and Mahley, R. W. (1981) *J. Biol. Chem.* **256**, 9077–9083
  17. Rall, S. C., Jr., Weisgraber, K. H., and Mahley, R. W. (1982) *J. Biol. Chem.* **257**, 4171–4178
  18. Aggerbeck, L. P., Wetterau, J. R., Weisgraber, K. H., Wu, C.-S. C., and Lindgren, F. T. (1988) *J. Biol. Chem.* **263**, 6249–6258
  19. Wetterau, J. R., Aggerbeck, L. P., Rall, S. C., Jr., and Weisgraber, K. H. (1988) *J. Biol. Chem.* **263**, 6240–6248
  20. Dong, L.-M., Wilson, C., Wardell, M. R., Simmons, T., Mahley, R. W., Weisgraber, K. H., and Agard, D. A. (1994) *J. Biol. Chem.* **269**, 22358–22365
  21. Dong, L.-M., and Weisgraber, K. H. (1996) *J. Biol. Chem.* **271**, 19053–19057
  22. Morrow, J. A., Segall, M. L., Lund-Katz, S., Phillips, M. C., Knapp, M., Rupp, B., and Weisgraber, K. H. (2000) *Biochemistry* **39**, 11657–11666
  23. Acharya, P., Segall, M. L., Zaiou, M., Morrow, J., Weisgraber, K. H., Phillips, M. C., Lund-Katz, S., and Snow, J. (2002) *Biochim. Biophys. Acta* **1584**, 9–19
  24. Ptitsyn, O. B. (1995) *Adv. Protein Chem.* **47**, 83–229
  25. Dobson, C. M. (2001) *Philos. Trans. R. Soc. Lond-Biol. Sci.* **356**, 133–145
  26. Gursky, O., and Atkinson, D. (1996) *Proc. Natl. Acad. Sci. U. S. A.* **93**, 2991–2995
  27. Weers, P. M. M., Kay, C. M., and Ryan, R. O. (2001) *Biochemistry* **40**, 7754–7760
  28. Barrick, D., and Baldwin, R. L. (1993) *Biochemistry* **32**, 3790–3796
  29. Oberg, K. A., and Fink, A. L. (1998) *Anal. Biochem.* **256**, 92–106
  30. Oberg, K. A., Ruyschaert, J.-M., Azarkan, M., Smolders, N., Zerhouni, S., Wintjens, R., Amrani, A., and Looze, Y. (1998) *Eur. J. Biochem.* **258**, 214–222
  31. Cabiaux, V., Oberg, K. A., Pancoska, P., Walz, T., Agre, P., and Engel, A. (1997) *Biophys. J.* **73**, 406–417
  32. Schmitz, K. S. (1990) in *An Introduction to Dynamic Light Scattering by Macromolecules*, Academic Press, Boston
  33. Spolaore, B., Bermejo, R., Zamboni, M., and Fontana, A. (2001) *Biochemistry* **40**, 9460–9468
  34. Wilson, C., Wardell, M. R., Weisgraber, K. H., Mahley, R. W., and Agard, D. A. (1991) *Science* **252**, 1817–1822
  35. Morrow, J. A., Arnold, K. S., and Weisgraber, K. H. (1999) *Protein Expr. Purif.* **16**, 224–230
  36. Segelke, B. W., Forstner, M., Knapp, M., Trakhanov, S. D., Parkin, S., Newhouse, Y. M., Bellamy, H. D., Weisgraber, K. H., and Rupp, B. (2000) *Protein Sci.* **9**, 886–897
  37. Lu, B., Morrow, J. A., and Weisgraber, K. H. (2000) *J. Biol. Chem.* **275**, 20775–20781
  38. Segall, M. L., Dhanasekaran, P., Baldwin, F., Anantharamaiah, G. M., Weisgraber, K. W., Phillips, M. C., and Lund-Katz, S. (2002) *J. Lipid Res.* **43**, 1688–1700
  39. Weisgraber, K. H. (1994) *Adv. Protein Chem.* **45**, 249–302
  40. Fisher, C. A., Narayanaswami, V., and Ryan, R. O. (2000) *J. Biol. Chem.* **275**, 33601–33606
  41. Weers, P. M. M., Narayanaswami, V., and Ryan, R. O. (2001) *Eur. J. Biochem.* **268**, 3728–3735
  42. DeMattos, R. B., Curtiss, L. K., and Williams, D. L. (1998) *J. Biol. Chem.* **273**, 4206–4212
  43. Nathan, B. P., Bellosta, S., Sanan, D. A., Weisgraber, K. H., Mahley, R. W., and Pitas, R. E. (1994) *Science* **264**, 850–852
  44. Nathan, B. P., Chang, K.-C., Bellosta, S., Brisch, E., Ge, N., Mahley, R. W., and Pitas, R. E. (1995) *J. Biol. Chem.* **270**, 19791–19799
  45. Holtzman, D. M., Pitas, R. E., Kilbridge, J., Nathan, B., Mahley, R. W., Bu, G., and Schwartz, A. L. (1995) *Proc. Natl. Acad. Sci. U. S. A.* **92**, 9480–9484
  46. Bellosta, S., Nathan, B. P., Orth, M., Dong, L.-M., Mahley, R. W., and Pitas, R. E. (1995) *J. Biol. Chem.* **270**, 27063–27071
  47. Fagan, A. M., Bu, G., Sun, Y., Daugherty, A., and Holtzman, D. M. (1996) *J. Biol. Chem.* **271**, 30121–30125
  48. Sun, Y., Wu, S., Bu, G., Onifade, M. K., Patel, S. N., LaDu, M. J., Fagan, A. M., and Holtzman, D. M. (1998) *J. Neurosci.* **18**, 3261–3272
  49. Poirier, J. (1996) *J. Psychiatry Neurosci.* **21**, 128–134
  50. Huang, Y., Liu, X. Q., Wyss-Coray, T., Brecht, W. J., Sanan, D. A., and Mahley, R. W. (2001) *Proc. Natl. Acad. Sci. U. S. A.* **98**, 8838–8843
  51. Ji, Z.-S., Miranda, R. D., Newhouse, Y. M., Weisgraber, K. H., Huang, Y., and Mahley, R. W. (2002) *J. Biol. Chem.* **277**, 21821–21828
  52. Sanan, D. A., Weisgraber, K. H., Russell, S. J., Mahley, R. W., Huang, D., Saunders, A., Schmechel, D., Wisniewski, T., Frangione, B., Roses, A. D., and Strittmatter, W. J. (1994) *J. Clin. Invest.* **94**, 860–869
  53. Ma, J., Yee, A., Brewer, H. B., Jr., Das, S., and Potter, H. (1994) *Nature* **372**, 92–94
  54. Wisniewski, T., Castaño, E. M., Golabek, A., Vogel, T., and Frangione, B. (1994) *Am. J. Pathol.* **145**, 1030–1035
  55. Wisniewski, T., and Frangione, B. (1992) *Neurosci. Lett.* **135**, 235–238